Journal Pre-proof

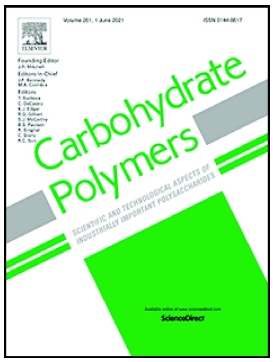

.Cinnamaldehyde-enriched Pickering emulsions stabilized by modified cellulose I and II nanocrystals recycled from maple leaves for shrimp preservation

Chuye Ji, Jiachen Wei, Yixiang Wang

PII: S0144-8617(23)01055-X

DOI: https://doi.org/10.1016/j.carbpol.2023.121590

Reference: CARP 121590

To appear in: *Carbohydrate Polymers*

Received date: 10 October 2023

Revised date: 10 November 2023

Accepted date: 11 November 2023

Please cite this article as: C. Ji, J. Wei and Y. Wang, .Cinnamaldehyde-enriched Pickering emulsions stabilized by modified cellulose I and II nanocrystals recycled from maple leaves for shrimp preservation, *Carbohydrate Polymers* (2023), https://doi.org/10.1016/j.carbpol.2023.121590

Cinnamaldehyde-enriched Pickering emulsions stabilized by modified cellulose I and II nanocrystals recycled from maple leaves for shrimp preservation

Chuye Ji, Jiachen Wei, Yixiang Wang*

Department of Food Science and Agricultural Chemistry, McGill University, Ste Anne de Bellevue, Quebec, Canada H9X 3V9

*Correspondence: yixiang.wang@mcgill.ca, +001(514)3987922

ABSTRACT: The utilization of biomass waste has attracted much interest, but such attention hasn't been paid to the abundant fallen maple leaves in Canada. Herein, we aim to obtain cellulose nanocrystals (CNCs) from maple leaves and explore their potential applications as sustainable stabilizers of Pickering emulsions for the preservation of food products with complicated structures. The results reveal that two types of CNCs were extracted from maple leaves at different alkaline conditions. Octenyl succinic anhydride was selected to modify rod-like CNCs, and the CNC-stabilized oil-in-water Pickering emulsions showed excellent stability. Cinnamaldehyde, a model antibacterial compound, was incorporated in the Pickering emulsions, which exhibited the improved storage stability and sustained antibacterial capacity towards both Gram-positive and Gram-negative bacteria. Shrimp was chosen as an example that has complicated surface structure and is hard to disinfect, and the CNC-stabilized Pickering emulsions could be easily sprayed on the surface of shrimp to inhibit the proliferation of bacteria and inactivate the psychrophilic bacteria responsible for shrimp spoilage at refrigerated condition, so as to preserve the quality

of shrimp. Therefore, the current work suggests the possibility to utilize fallen maple leaves as a promising source of CNCs and the applications of CNC-stabilized Pickering emulsions in seafood preservation.

KEYWORDS: Pickering emulsions; maple leaves; cellulose I and II nanocrystals; modification; shrimp preservation

1. INTRODUCTION

Fallen maple leaves as "green waste" are abundant in Canada. They are composed of a variety of compounds including carbohydrates, lipids, proteins, minerals, and so on, and are a potential low-cost source of quality cellulose. Cellulose nanocrystals (CNCs) have been widely applied in food packaging, emulsion stabilization, quality sensor, and food thickener, and there is an increasing trend to obtain CNCs from waste biomass (Huang, Liu, Chang, & Wang, 2020). The extraction of CNCs usually consists of pretreatments (removal of contaminations and soluble substances), purifications (removal of hemicellulose and lignin), and fragmentation (generation of nanostructure via hydrolysis) (Dai, et al., 2020). To our knowledge, there is no report involving the preparation of CNCs from maple leaves and their value-added application in food preservation.

CNCs have emerged as sustainable stabilizers/emulsifiers in food-related Pickering emulsions owing to their favorable properties such as biocompatibility, renewability, low toxicity, and high aspect ratio (Dai, et al., 2020). The irreversible adsorption of CNCs at oil/water interface prevents the Pickering emulsion droplets from coalescence (Binks, 2002). The ability of CNCs to stabilize emulsions varies with

their source, morphology, surface chemistry, and other factors (Cherhal, Cousin, & Capron, 2016; Kalashnikova, Bizot, Cathala, & Capron, 2012; Li, et al., 2018). CNCs with different crystalline allomorphs have different properties including surface charge, thermal stability, and dispersibility (Gong, Mo, & Li, 2018). However, very few research works compared the emulsifying capacities of CNCs with different crystalline allomorphs (Haouache, et al., 2022a; Li, et al., 2018). Typically, native cellulose I has the parallel packing of cellulose chains and can be irreversibly converted into cellulose II with the antiparallel chain arrangement and intersheet hydrogen bonding by mercerization or regeneration (Sarko & Muggli, 1974; Zugenmaier, 2001). Li et al. reported that cellulose I nanocrystals (CNC I) had a better ability to stabilize oil-in-water emulsions than cellulose II nanocrystals (CNC II), but the CNC II they used was ellipsoid-shaped with a low aspect ratio of 1.7 and was 11 times shorter than the CNC I, making the comparison complicated (Li, et al., 2018). Haouache et al. (2022a) stated that CNC I and CNC II oriented their hydrophobic surfaces (010 and 100, respectively) to the oil/water interface, where CNC I formed a uniform and concentration-independent interfacial layer via face-on adsorption, and CNC II generated a thicker and rougher layer via edge-on adsorption. However, in the practical situation, the emulsification performance of pristine CNCs suffers from their high hydrophilicity (Cherhal, et al., 2016). Therefore, it is necessary to study the effect of surface modification of CNCs on the affinity and arrangement of CNCs with different crystalline allomorphs at the oil-water interface. Various modifications have been applied to improve the surface hydrophobicity of CNCs

(Pang, et al., 2020; Tang, et al., 2019). Among them, octenyl succinic anhydride (OSA) has been used for decades in food industry for the modification of starch (Sweedman, Tizzotti, Schäfer, & Gilbert, 2013), and the OSA-modified starch has been permitted in foods at a level of 3.0 wt% by Food and Drug Administration (FDA). In recent years, OSA modification of cellulose for Pickering emulsion formulations has attracted increasing interest (Chen, et al., 2018; Du Le, Loveday, Singh, & Sarkar, 2020; Gao, et al., 2022; Xie, et al., 2020), but the comparison of OSA-modified CNCs with different crystalline allomorphs has not yet been reported.

Seafood is highly perishable with limited shelf life because of the melanosis and microbial spoilage (Olatunde, Tan, Shiekh, Benjakul, & Nirmal, 2021). Traditional sulfiting agents as preservatives may pose a risk to human health, and the complicated surface structure of seafood makes it hard to disinfect. Therefore, in this study, we hypothesize that fallen maple leaves can be a promising source of CNCs and the obtained CNCs can act as the stabilizers of Pickering emulsions loaded with antibacterial compounds for seafood preservation. Cinnamaldehyde, a hydrophobic aromatic aldehyde, was selected as a model without safety concerns at the proposed levels of intake and has strong antibacterial activity to inhibit the growth of Gram-positive and Gram-negative bacteria (Chen, et al., 2017; Cocchiara, Letizia, Lalko, Lapczynski, & Api, 2005; Muhoza, et al., 2023; Rieger & Schiffman, 2014; Shen, et al., 2015). The encapsulation and storage stability of cinnamaldehyde in the Pickering emulsions stabilized by OSA-modified CNCs were evaluated, and the antibacterial activity was examined by spray coating the emulsions on fresh white shrimp.

2. EXPERIMENTAL SECTION

2.1. Materials

Maple leaves were collected from Macdonald Campus of McGill University (Ste Anne de Bellevue, QC, Canada). Octenyl succinic anhydride (OSA, $C_{12}H_{18}O_3$, 97%) were purchased from MilliporeSigma Canada Ltd. (Oakville, ON, Canada). Canola oil was purchased from Costco Wholesale store in Montreal (QC, Canada). Luria-Bertani (LB) medium, plate count agar (PCA), Cetrimide agar base (CAB) for *Pseudomonas aeruginosa*, and tryptic soy agar (TSA) were purchased from Becton Dickinson (Franklin Lakes, NJ, USA). Peptone water was obtained from Oxoid Ltd. (Ottawa, ON, Canada). Trans-cinnamaldehyde (99%), sulfuric acid (H_2SO_4, 95%-98%), sodium chlorite ($NaClO_2$, 80%), sodium hydroxide (NaOH, ≥97%), ethanol, methanol, acetone, and all other solvents and chemicals were of reagent grade and obtained from Fisher Scientific (Ottawa, ON, Canada).

2.2. Isolation of cellulose I and II from maple leaves

The collected maple leaves were washed with water, oven-dried at 50°C, and grounded into powder by using a commercial miller (F203 blade grinder, Krups, Solingen, Germany) to pass through a 60-mesh sieve. The finely grinded powder was dewaxed in a Soxhlet apparatus system with acetone at 70°C for 12 h, and delignified with 1.7% (w/v) $NaClO_2$ solution at pH 4 and 75°C for 5 h. Afterwards, the alkali treatment was conducted with 5 wt% NaOH at 80°C for 2 h or with 17.5 wt% NaOH at 25°C for 45 min to obtain cellulose I or II, respectively (Corrêa, de Morais Teixeira,

Pessan, & Mattoso, 2010). The insoluble residue (cellulose I or II) was washed with distilled water and freeze-dried (Labconco FreeZone 12L-50C, Labconco Corporation, Kansas, MO, USA) for further use. The determination of main constituents of the obtained cellulose I and II was performed according to the following ASTM standard methods: ASTM D1106-96 for lignin, ASTM D1104-56 for holocellulose, and ASTM D 1103-60 for α-cellulose. The yields of cellulose I and II were 18.65%±1.03% and 17.14%±0.87%, respectively.

2.3. Preparation and characterization of CNC I and II

Cellulose (type I or II, 5 g) was mixed with 100 mL of 64 wt% H_2SO_4 solution at 45°C under constant stirring at 400 rpm for 20, 40, and 60 min, respectively. The hydrolysis was terminated by adding 10-fold cold distilled water, and the suspension was washed with distilled water by multiple centrifugations at 6,000 ×g for 10 min and then dialyzed for 72 h to remove H_2SO_4 and hydro-soluble residues. The yields of CNC I and II with different hydrolysis times were calculated as a mass percentage relative to their original cellulose masses.

The morphology of CNCs was observed by Talos F200X G2 TEM (Thermo Fisher Scientific Inc., Waltham, MA, USA). Diluted CNC suspension (5 μL) was deposited on a carbon-coated copper grid for 5 min. The grid was then stained with 2% aqueous uranyl acetate (5 μL) for 60 s. After air drying at room temperature, the negatively stained CNC samples were imaged on TEM at a voltage of 200 kV. The geometrical aspects of CNCs were measured using digital image analysis (ImageJ software, Bethesda, MD, USA). For each sample, over three images were selected and over 100

particles per image were measured.

XRD patterns of CNCs were obtained using an Empyrean X-ray diffractometer (Malvern Panalytical Ltd., Malvern, Worcs, UK) equipped with a Bragg Brentano configuration and Cu/Kα radiation. The crystallinity index (CrI) was determined using the peak height method (Azubuike, Rodríguez, Okhamafe, & Rogers, 2012):

$$CrI(\%) = (1-\frac{I_{am}}{I_{Cr}})\times 100\% \quad (1)$$

where I_{Cr} is the maximum diffraction intensity associated with surface areas of crystalline cellulose (at 2θ of 22.8° for cellulose I and at 2θ of 21.8° for cellulose II), and I_{am} is the diffraction intensity attributed to amorphous cellulose (at 18° for cellulose I and at 16° for cellulose II) (Azubuike et al., 2012).

FTIR spectra of CNCs were recorded by using a Cary 630 FTIR spectrometer with an attenuated total reflectance sampling module (Agilent technologies Inc., Santa Clara, CA, USA). The spectra were measured in the range from 4000 to 650 cm^{-1} as the average of 64 scans with a resolution of 2 cm^{-1}, using the empty accessory as blank.

2.4. OSA modification of CNCs

OSA modification of CNCs was performed according to the method of Du Le et al. (2020) with some modifications. The CNC suspension (2.0 wt%, hydrolysis time of 40 min) was mixed with OSA at mass ratios of 1.0:0.2, 1.0:0.5, and 1.0:1.0, respectively, and the pH was maintained at 8.3 by the continuous addition of 0.5 M NaOH. Once the reaction was complete, the suspensions were adjusted to pH 7.0 using 0.1 M HCl and freeze-dried. The freeze-dried powders were washed with

ethanol at least three times and then oven-dried at 50°C overnight to remove ethanol. The obtained modified CNC I and II were coded as CNC I-0.2 OSA, CNC I-0.5 OSA, CNC I-1.0 OSA, CNC II-0.2 OSA, CNC II-0.5 OSA, and CNC II-1.0 OSA, respectively, based on the mass ratios of OSA to CNC.

The degree of substitution (DS) in OSA-modified CNCs was determined by direct titration method (Ruan, Chen, Fu, Xu, & He, 2009; Liu, Sun, Zhang, Ren, & Geng, 2006). The DS was calculated using Eq. (2):

$$DS = \frac{162 \times n_{COOH}}{m - 210 \times n_{COOH}} \quad (2)$$

where 162 g mol^{-1} is the molar mass of an anhydroglucose unit (AGU), 210 g mol^{-1} is the net increase in the mass of an AGU for each OSA substituted, m is the dry weight (g) of OSA-modified CNC sample, and n_{COOH} is the amount (mol) of COOH calculated from the titration.

2.5. Cinnamaldehyde-loaded Pickering emulsions stabilized by CNCs

Both unmodified and OSA-modified CNCs were used to stabilize Pickering emulsions. The mixture of canola oil, water, and CNCs was homogenized at 25,000 rpm for 3 min using an Ultra Turrax T25 high-speed homogenizer (IKA, BW, Germany). The concentration of CNCs was 1.0% (w/v), and the volume fraction of oil phase was 10% (v/v). Cinnamaldehyde-loaded Pickering emulsions (CA/PE) were prepared by dissolving cinnamaldehyde (100 mg/mL) in oil phase and stabilized by CNC I-0.5 OSA. Size distribution and ζ-potential of CNCs and Pickering emulsions were measured at 25°C using a NanoBrook Omni Particle Size and ζ-Potential Analyzer (Brookhaven Instruments Ltd, Holtsville, NY, USA). The cream layer of

Pickering emulsions was observed using the LMC-1000 optical microscope equipped with a digital camera (Laxco, Mill Creek, WA, USA).

Freshly prepared cinnamaldehyde-loaded Pickering emulsions were centrifuged at 13,000 ×g for 0.5 h at 4°C using Eppendorf 5424 centrifuge (Eppendorf Co. Ltd, Hamburg, Germany). The contents of cinnamaldehyde in the whole emulsion (C_w) and in the subnatant (C_s) were determined by liquid-liquid extraction method (Cheng, et al., 2020; Wang, et al., 2016). Briefly, 1 mL of emulsion or subnatant was mixed with 1 mL of ethanol under vortex for 1 min. Cinnamaldehyde was extracted by adding 4 mL of methanol under vortex for 2 min and then centrifuged at 3,000 ×g for 5 min at 4°C. Cinnamaldehyde contents in the supernatants were determined at 285 nm on a Hitachi UV-2000 UV-visible spectrophotometer (Hitachi, Tokyo, Japan), and the encapsulation efficiency was calculated from the difference between C_w and C_s divided by C_w.

Cinnamaldehyde-loaded Pickering emulsions were stored in an incubator at 25°C and the contents of cinnamaldehyde were analyzed during storage for 0, 7, 14, 21, and 28 days. The retention of cinnamaldehyde was described as a percentage relative to the initial cinnamaldehyde content.

2.6. Antibacterial test

The antibacterial activity was evaluated by using the Gram-positive bacteria *S. aureus* ATCC 6538 and the Gram-negative bacteria *E. coli* K12 as the model microbes. Each bacterial strain was prepared from glycerol stock (20%, v/v) and streaked for isolation on TSA plates. The plates were incubated at 37°C for 24 h, and

then the isolated colonies were cultivated in 4 mL of LB broth at 37°C with constant shaking at 175 rpm for 16 h. The culture solutions with a concentration of ~10^8 CFU/mL of *S. aureus* and *E. coli* were achieved.

The minimal inhibitory concentrations (MICs) of cinnamaldehyde alone and CA/PE were determined by standard broth microdilution susceptibility testing assay as described in the previous studies (Cheng, et al., 2020; Shi, et al., 2017) with a few modifications. Antibacterial agents (cinnamaldehyde and CA/PE) were diluted to 10, 5, 2.5, 1.0, 0.5, and 0.05 mg/mL of cinnamaldehyde with sterile LB broth and mixed with same volume of bacterial suspensions (1×10^8 CFU/mL). The MIC value was defined as the minimum concentration of antimicrobial that inhibited more than 90% of the microorganism's growth after incubation for 24 h at 37°C (Andrews, 2001), while the minimum bactericidal concentration (MBC) was the minimum concentration of antimicrobial required to kill the bacteria after incubation at the same conditions and colonies did not grow when subculturing the samples on agar plates (Li, et al., 2019).

The zone of inhibition was measured using the well diffusion method (Mikulcová, Bordes, & Kašpárková, 2016). *S. aureus* and *E. coli* suspensions (~10^8 CFU/mL) were evenly spread on LB agar plates. The wells (diameter of 6 mm) were carved using a sterile borer and filled with 100 μL of undiluted emulsions. Sterile distilled water was employed as the control. The diameter of the bacterial inhibition zone was measured after 24 h of incubation at 37°C. The zone of inhibition of CA/PE during storage at 25°C was analyzed on days 0, 7, 14, 21, and 28.

2.7. Shrimp preservation test

White shrimp meat pieces (25 g), purchased from a local market (Montreal, QC, Canada), were sterilized by ethanol, and then burnt and trimmed. They were inoculated with *P. aeruginosa* PA14 suspension (~10^6 CFU/mL) for 30 min to allow bacteria fixation. The final concentration of *P. aeruginosa* on shrimp samples reached around 10^5 CFU/g. Subsequently, the inoculated samples were mixed with cinnamaldehyde alone and CA/PE at a ratio of 10:1 (w/w), respectively, and were stored in sterile filter bags at 4°C for 10 days. The *P. aeruginosa* count was determined at 1, 3, 6, and 10 days of storage. The samples (25 g) were mixed with 225 mL of 0.1% peptone water and homogenized in a Stomacher Lab-Blender 400 (Gemini Techniek B.V., Haaksbergen, CV, Netherlands) for 2 min. Then, 100 µL of appropriate sample dilutions were spread onto CAB plates for 24 h of incubation at 37°C.

Microbiological analysis was performed by spread plate method (Ibrahim Sallam, 2007). The CA/PE was loaded in a commercial spray bottle to spray-coat the surface of whole head-on shrimps. The shrimps with/without CA/PE coating were stored at 4°C, and the total viable count (TVC) and psychrophilic bacterial count (PBC) were determined every 3 days (Sae-leaw & Benjakul, 2019). Briefly, 25 g of shrimp meat were mixed with 225 mL of 0.1% peptone water and homogenized for 2 min. Ten-fold serial dilutions of the homogenate in 0.1% peptone water were conducted, and 100 µL of appropriate sample dilutions were spread onto PCA plates and incubated at 37°C and 4°C for 2 and 5 days, respectively.

Melanosis analysis of shrimps was carried out according to the previous studies (Li, et al., 2022; Nirmal & Benjakul, 2009). The melanosis score was determined through visual inspection by 10-point scale, where a score of 0 indicated absent and 10 indicated extremely severe.

2.8. Statistical analysis

All experiments were conducted in triplicate with data reported as the mean ± standard deviation. The mean values were analyzed for a significant difference (p< 0.05) by using the SPSS statistics 26.0 software package (IBM, Armonk, NY, USA).

3. RESULTS AND DISCUSSION

3.1. Structure of CNC I and II with/without OSA modification

The chemical compositions of maple leaf cellulose I and II are listed in Table S1, and their yields were around 18.65% and 17.14%, respectively. The morphology of CNC I and II with different hydrolysis times is shown in Fig. 1A, and their dimensions are summarized in Table 1. Both CNC I and II exhibited a typical rod-like shape, while CNC II was significantly shorter and had a lower aspect ratio than CNC I (Gong, et al., 2018). It was due to the penetration of alkali in the native crystalline region of cellulose I, disrupting the interchain contacts and subsequently inducing the formation of the bioriented cellulose II structure upon alkali removal, which had a significant impact on the crystal organization with a lower chain packing per nanocrystal and a lower degree of polymerization in cellulose II (Haouache, et al., 2022b; Ko, et al., 2018). The hydrolysis time had no significant effect on the

morphology and dimensions of CNC I (Kargarzadeh, et al., 2012), but the mean length of CNC II reduced from 104.0±27.3 nm (hydrolysis time of 20 min) to 66.7±13.3 nm (hydrolysis time of 40 min), indicating that a short hydrolysis time of 20 min was insufficient for the removal of the increased amorphous region during the mercerization process (Schenzel, Almlöf, & Germgård, 2009). As the hydrolysis time further increased to 60 min, there was no significant influence on the dimensions of CNC II, because the crystalline region is more stable than the amorphous region during hydrolysis (Li, Li, Zou, Zhou, & Lian, 2014). The yields of CNC I and II with the hydrolysis time of 20 min were the lowest, and there was no significant difference between the yields when the hydrolysis times were 40 and 60 min. The yield of around 20% (for both CNC I and II) was comparable to the previously reported samples obtained by sulfuric acid (64 wt%) hydrolysis from pine cone cellulose and Tetra pak cellulose (García-García, Balart, Lopez-Martinez, Ek, & Moriana, 2018; Xing, Gu, Zhang, Tu, & Hu, 2018).

Fig. 1B illustrates the XRD patterns and crystallinity of CNC I and II. CNC I exhibited the typical peaks of cellulose I at 22.8°, 14.9°, and 16.4° (French & Santiago Cintrón, 2013), while CNC II had the characteristic diffraction peaks of cellulose II at 12°, 20°, and 21.8° (French, 2014). Fig. 1C shows the FTIR spectra of CNC I and II with hydrolysis times of 20, 40, and 60 min, respectively. Cellulose characteristic peaks were observed in the spectra of CNC I at around 3335, 2900, and 1060 cm^{-1}, corresponding to the stretching vibration of O−H, C−H, and C−O bond distortion in glucoside, respectively. Compared to CNC I, the spectra of CNC II

displayed two distinctive peaks at 3490 and 3443 cm^{-1}, relating to the intramolecular hydrogen bonding stretching vibration of cellulose II (Flauzino Neto, et al., 2016; Li, et al., 2014). The absorbance of C−H stretching shifted to 2890 cm^{-1}, which was also assigned to cellulose II (Li, et al., 2014). The symmetric bending vibration peak of CH_2 at 1428 cm^{-1} shifted to 1419 cm^{-1}, owing to the change in the conformation of hydroxymethyl groups from *tg* to *gt* (Flauzino Neto, et al., 2016; Han, Zhou, Wu, Liu, & Wu, 2013), while the stretching vibration peak of C−O at C_6 shifted from 1033 cm^{-1} in CNC I to 1016 cm^{-1} in CNC II (Xing, Hu, Zhang, Guan, & Gu, 2020). Moreover, the asymmetric stretching vibration peak of C−O−C at β-glycosidic linkage was switched from 898 cm^{-1} in CNC I to 894 cm^{-1} in CNC II, which might be due to the changes in the torsional angles of β-glycosidic linkage (Flauzino Neto, et al., 2016; Xing, et al., 2020). These results further confirmed the different crystalline allomorphs of CNC I and II. No shift of adsorption peaks was observed upon increasing hydrolysis time from 20 min to 60 min, indicating that the structures of CNCs were retained. Considering the above-mentioned features, the hydrolysis time of 40 min was selected to prepare CNC I and II for the following studies.

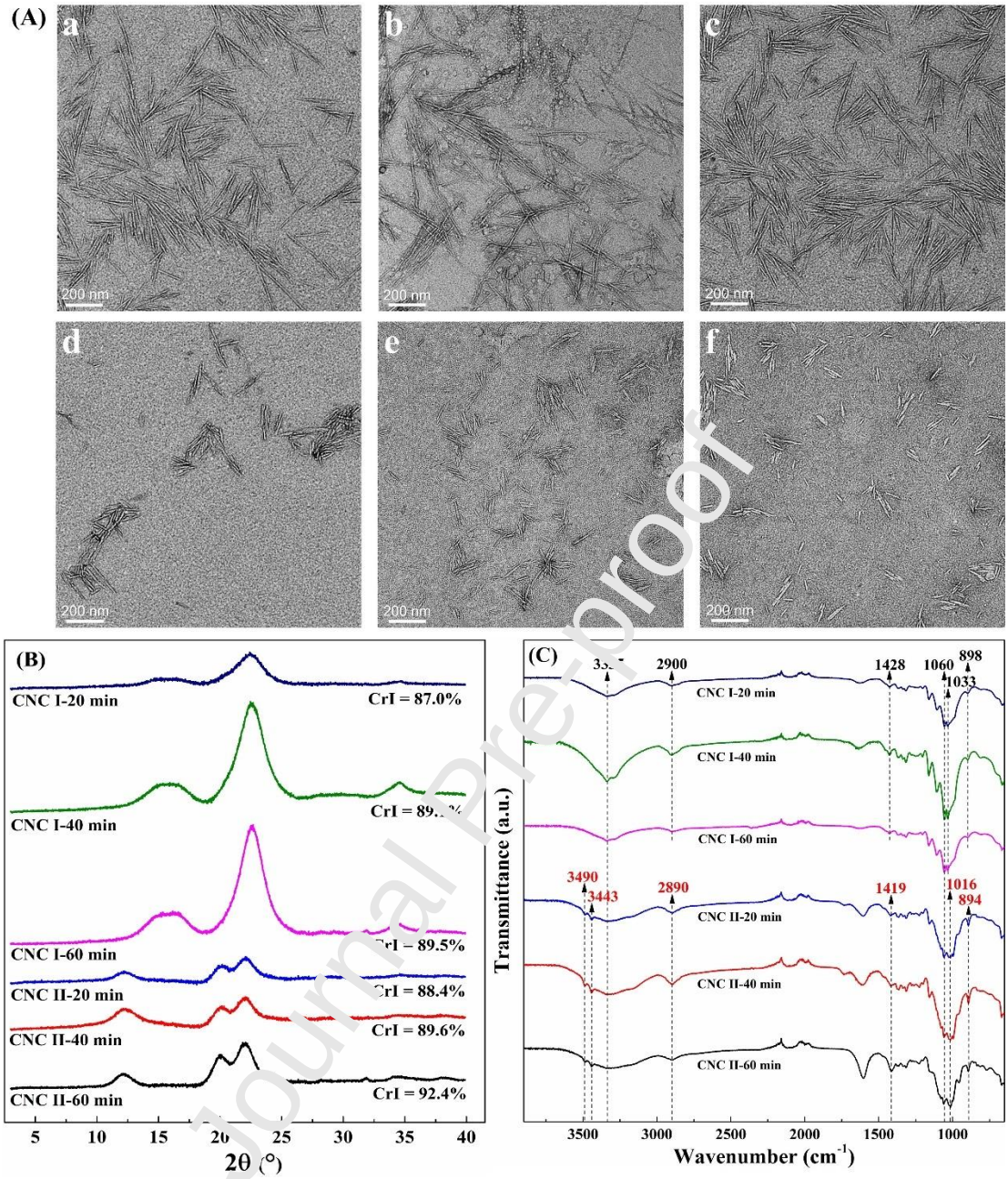

Fig. 1 (A) TEM images of CNC I (top) and CNC II (bottom) with reaction time of 20 min (a, d), 40 min (b, e), and 60 min (c, f). (B) XRD patterns and (C) FTIR spectra of CNC I and II with different reaction times.

Table 1. Particle size and yield rate of CNC I and CNC II with different reaction times.

CNC	Reaction time (min)	Length (nm)	Diameter (nm)	Aspect ratio	Yield rate (%)

CNC I	20	211.3 ± 20.7^{c}	12.4 ± 1.4^{ab}	16.24 ± 1.74^{b}	10.63 ± 1.21^{a}
	40	220.5 ± 22.0^{c}	13.0 ± 2.9^{b}	17.56 ± 3.49^{b}	20.31 ± 1.23^{b}
	60	224.8 ± 18.8^{c}	13.7 ± 3.6^{b}	17.37 ± 4.41^{b}	20.01 ± 1.06^{b}
CNC II	20	104.0 ± 27.3^{b}	9.7 ± 2.3^{ab}	10.79 ± 2.77^{ab}	12.51 ± 1.66^{a}
	40	66.7 ± 13.3^{a}	6.5 ± 1.1^{a}	10.50 ± 2.37^{ab}	19.67 ± 0.68^{b}
	60	64.9 ± 13.6^{a}	8.4 ± 1.7^{ab}	7.91 ± 1.69^{a}	19.95 ± 0.91^{b}

Notes: Different letters represent statistically significant difference (p<0.05).

The OSA groups are generally introduced to CNCs through the esterification reaction (Chen, et al., 2018). As shown in Fig. 2, the FTIR spectra of OSA-modified CNCs had a significant new peak at 1568 cm^{-1} that was assigned to the asymmetric stretching vibration of carboxylate $RCOO^{-}$ (Quintero-Castaño, et al., 2020). The characteristic peaks at 2924, 2856, and 1451 cm^{-1} assigned to the alkyl chains were also observed in the OSA-modified CNCs. The Intensities of these peaks became stronger with the increase of OSA concentrations, which was consistent with the higher degree of substitution (DS) (listed in Table 2) (Takihara, Yoshida, & Isogai, 2007; Wang, He, Huang, Luo, & Fu, 2013). Similar results were reported for OSA-modified starches (Quintero-Castaño, et al., 2020; Zainal Abiddin, Yusoff, & Ahmad, 2018), but the different allomorphs of CNCs had no significant effects on the DS values. The changes in the surface charge of CNCs and OSA-modified CNCs are listed in Table 2. The unmodified CNCs were negatively charged owing to the sulfate groups induced by sulfuric acid hydrolysis, and the ζ-potential (at pH 7.0) of CNC I and II were −35.46±1.54 and −32.89±2.26 mV, respectively, which were similar to

those of asparagus CNCs (–31 mV) (Wang, et al., 2016) and lemon seed CNCs (–36 mV) (Dai, et al., 2021). The OSA-modified CNCs showed greater magnitudes of ζ-potential due to the introduction of $–COO^-$ groups (Chen, et al., 2018).

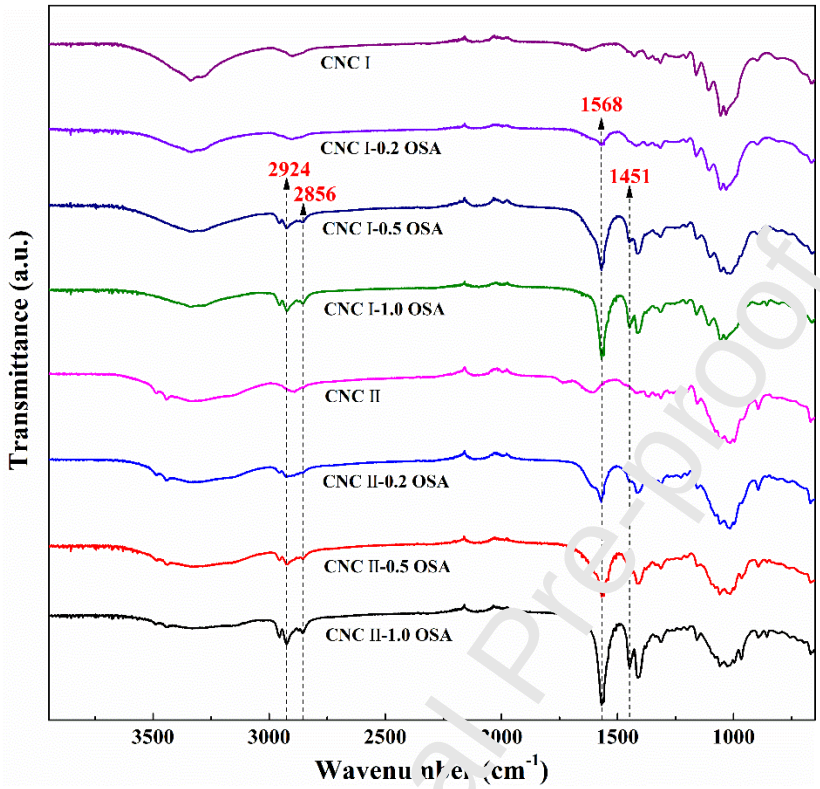

Fig. 2 FTIR spectra of unmodified and OSA-modified CNC I and II.

Table 2 Degree of substitution and ζ-potential of OSA-modified CNCs with different mass ratios of OSA to CNC (0, 0.2, 0.5, and 1.0).

CNC	Ratio of OSA to CNC	Degree of substitution	ζ-Potential (mV)
CNC I	0	–	$–35.46 \pm 1.54^{ab}$
	0.2	0.0045 ± 0.0005^{a}	$–41.14 \pm 2.73^{bc}$
	0.5	0.0102 ± 0.0004^{b}	$–43.03 \pm 2.68^{c}$
	1.0	0.0187 ± 0.0008^{c}	$–44.27 \pm 1.49^{c}$
CNC II	0	–	$–32.89 \pm 2.26^{a}$
	0.2	0.0040 ± 0.0003^{a}	$–38.97 \pm 2.44^{abc}$

	0.5	0.0095 ± 0.0006^{b}	-40.81 ± 2.31^{bc}
	1.0	0.0191 ± 0.0006^{c}	-41.73 ± 1.77^{c}

Notes: Different letters represent statistically significant difference ($p<0.05$).

3.2. Pickering emulsions stabilized by OSA-modified CNC I and II

The Pickering emulsions stabilized by unmodified and modified CNC I and II were observed and compared. As shown in Fig. 3A, the droplets stabilized by unmodified CNC I were larger and less uniform than the ones stabilized by unmodified CNC II. It was because the CNC II particles were thinner and shorter and could be more easily organized at the oil-water interface (Haouache, et al., 2022a). However, both the emulsions stabilized by unmodified CNC I and II were unstable against coalescence because of the high hydrophilicity and poor wettability of CNCs (Cherhal, et al., 2016; Kalashnikova, et al., 2012). It was worth noting that the emulsions stabilized by 0.2 OSA and 0.5 OSA-modified CNCs had smaller and more homogeneous droplets than the unmodified samples. It was because the OSA modification could promote CNC particles to absorb on the oil-water interface to prevent aggregation and coalescence (Du Le, et al., 2020). Specifically, the emulsions stabilized by CNC I-0.2 OSA displayed two peaks at around 515 nm and 3328 nm (Table S2) and the ζ-potential value of –51 mV, while the CNC I-0.5 OSA PE sample had one uniform size distribution at 2954 nm (Table S2) and a higher ζ-potential of –66 mV. It indicated that the ratio of OSA to CNC I (0.5:1.0) could better improve the emulsification performance of CNC I (Chen, et al., 2018) and enhance the electrostatic repulsion

among oil droplets (Miao, et al., 2014). However, the emulsion droplets stabilized by OSA-modified CNC II showed the increased sizes and lower ζ-potential values when the mass ratio of OSA to CNC II changed from 0.2:1.0 to 0.5:1.0, suggesting the decreased loads of modified CNC II on the oil droplet surface (Zou, van Baalen, Yang, & Scholten, 2018). Similar results were observed in the emulsions stabilized by corn starch nanocrystals (Javidi, Razavi, & Mohammad Amini, 2019). With a further increase in the ratio of OSA to CNC to 1.0:1.0, the emulsion droplets became ununiform. It might be due to the strong hydrophobic interactions among the modified CNCs in the continuous phase and at the oil-water interface, which could contribute to the formation of compact clusters and result in the insufficient stabilizers (Foo, Ooi, Tan, & Chew, 2022; Zou, et al., 2018).

Fig. 3D shows the stability of the Pickering emulsions during storage. Phase separation with a clear oil layer occurred in the freshly prepared emulsions stabilized by unmodified CNC I and II. After 1 day of storage, oiling-off on top of the emulsions stabilized by CNC I-0.2 OSA was observed and resulted in a clear oil layer, while the CNC I-1.0 OSA PE sample exhibited the separated emulsion layer and the serum layer. CNC I-1.0 OSA particles tended to form aggregates via strong hydrophobic interactions, which induced the attachment between the CNC layers of neighboring droplets and resulted in the separation of emulsions during storage (Ko & Kim, 2021). All the emulsions stabilized by unmodified and modified CNC II showed the creaming layer on the top zone after preparation. Similar results were reported in the Pickering emulsions prepared by OSA-modified sweet potato residue cellulose (Xie,

et al., 2020). Especially, CNC II-1.0 OSA PE exhibited a relatively thicker creaming layer due to the increased interaction and droplet size (Melgosa, Benito-Román, Sanz, de Paz, & Beltrán, 2019). During 28 days of storage, the demulsification and delamination processes were observed in the Pickering emulsions prepared by OSA-modified CNC II. Notably, CNC I-0.5 OSA PE displayed outstanding long-term stability with the nearly unchanged droplet size of 3593 nm and the ζ-potential value of -61 mV after 28 days of storage, and the emulsion droplets were stable against aggregation, creaming, and oiling off (Fig. 3D & S2). It was due to the strong electrostatic repulsive force and the high physical stability. The sizes of the emulsion droplets should be theoretically equal to the diameter of oil droplets and two-fold thickness of CNC layer (Cheng, et al., 2020). Therefore, the thickness of the CNC I-0.5 OSA layer could be calculated to be around 430 nm. This value was much larger than the size of the individual OSA-modified CNC particle (Fig. S1), suggesting the formation of the thick CNC network to provide physical protection (Haouache, et al., 2022a; Javidi, et al., 2019; Lu & Tian, 2021; Zou, et al., 2018). Therefore, CNC I-0.5 OSA PE was selected for the following studies.

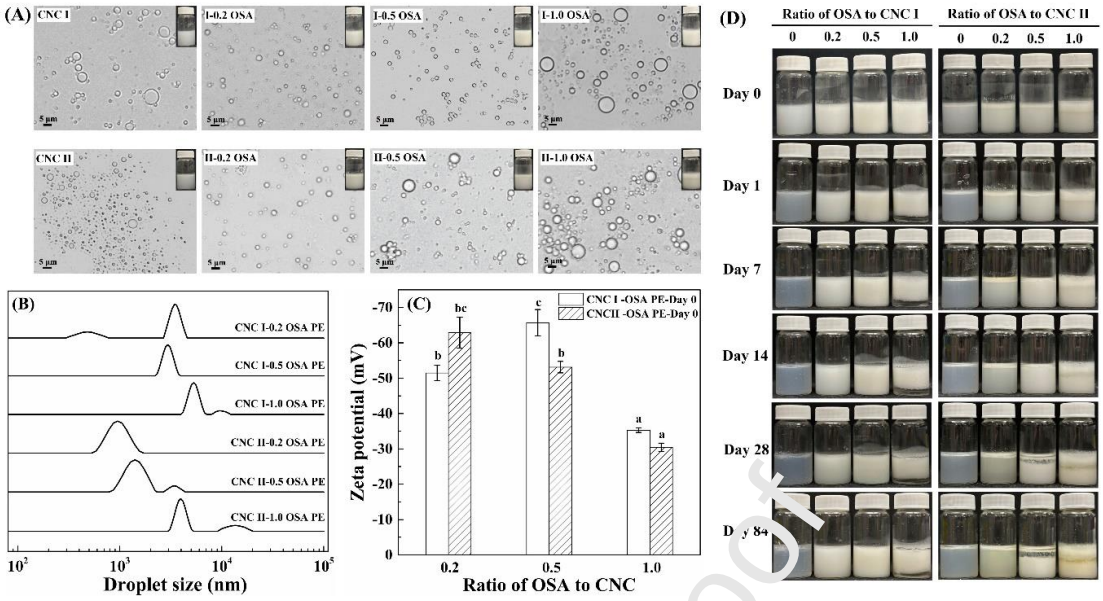

Fig. 3. Optical microscope images (A), size distribution (B), ζ-potential (C), and visual observation during storage (D) of the Pickering emulsions stabilized by OSA-modified CNC I and II. Different letters represent statistically significant difference (p<0.05).

3.3. Encapsulation efficiency and stability of cinnamaldehyde

The encapsulation efficiency of cinnamaldehyde in the Pickering emulsion stabilized by CNC I-0.5 OSA was 80.77%±2.09%, and the mass ratio of emulsifier and cinnamaldehyde was 1:1. This encapsulation efficiency was similar to that of cinnamaldehyde in the emulsions stabilized by Tween 20 (about 78%) at the emulsifier/cinnamaldehyde mass ratio of 3:1 (Jo, et al., 2015). Cinnamaldehyde is a hydrophobic aromatic aldehyde obtained from cinnamon plants and is prone to volatilize and easily oxidize during storage (Muhoza, et al., 2023; Wang, et al., 2021). As shown in Fig. 4, the retention of cinnamaldehyde control sharply decreased to 7% after storage at 25°C for 21 days, while the loss of cinnamaldehyde was much slower

in the Pickering emulsion stabilized by CNC I-0.5 OSA, with 52% remaining after 28 days. The result was comparable to cinnamaldehyde loaded in solid lipid nanoparticles, which could retain 52.36% after 15 days (Chen, et al., 2022). The modified CNCs provided a physical barrier at the oil-water interface and ensured the stability of emulsions. The encapsulation of cinnamaldehyde in the emulsion droplets reduced the accessibility to environmental factors and improved the storage stability (Cheng, et al., 2020).

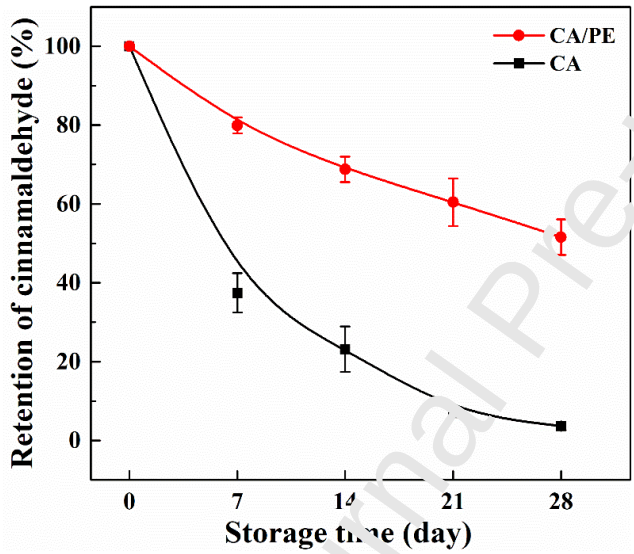

Fig. 4. Retention of cinnamaldehyde alone (CA) and cinnamaldehyde encapsulated in CNC I-0.5 OSA stabilized Pickering emulsion (CA/PE) during storage at 25°C.

3.4. Antibacterial activity

The MIC and MBC values of cinnamaldehyde alone and cinnamaldehyde-loaded emulsions are presented in Table 3. Cinnamaldehyde could interact with bacterial cell membranes via hydrophobic interactions, resulting in the increased permeability of the cell membranes and the enhanced leakage of cytoplasmic contents, and thus

destructing the cell structure (Han, et al., 2021; Shen, et al., 2015). MICs and MBCs of cinnamaldehyde alone for both Gram-positive (*S. aureus*) and Gram-negative (*E. coli*) bacteria were 1.0 and 2.5 mg/mL, respectively. However, the cinnamaldehyde-loaded emulsions displayed higher inhibitory effect on *S. aureus* (MIC and MBC of 1.0 mg/mL) than *E. coli* (MIC and MBC of 2.5 mg/mL). The antibacterial activity of the emulsions loaded with antibacterial agents is related to the droplet size and surface charge, which may influence the transport of antibacterial agents to cell membranes and their interactions with the multiple molecular cites at cell membranes (Cheng, et al., 2020; Donsì & Ferrari, 2016). *E. coli* has more negative charges than *S. aureus* due to the negatively charged lipopolysaccharides on the outer membrane of Gram-negative bacteria (Domingues, et al. 2014). The presence of the emulsion droplets with high negative surface charges could hinder the adhesion to Gram-negative bacteria (Domingues, et al., 2014; Gottenbos, Grijpma, van der Mei, Feijen, & Busscher, 2001).

Table 3. MIC and MBC of cinnamaldehyde alone (CA) and cinnamaldehyde-loaded Pickering emulsion stabilized by CNC I-0.5 OSA (CA/PE) against *E. coli* and *S. aureus* bacteria.

	MIC (mg/mL)		MBC (mg/mL)	
	CA	CA/PE	CA	CA/PE
E. coli	1.0	2.5	2.5	2.5
S. aureus	1.0	1.0	2.5	1.0

Additionally, the antibacterial activity of cinnamaldehyde-loaded emulsions was also determined using the well diffusion method and expressed in terms of the size of inhibition zone. As shown in Fig. 5, the cinnamaldehyde-loaded emulsions exhibited inhibitory activity against both *S. aureus* and *E. coli*, while no antibacterial effect was observed for the emulsions without cinnamaldehyde. The diameters of inhibition zones against *S. aureus* were larger than *E. coli* (as listed in Table 4), suggesting a better effect on inhibiting the growth of Gram-positive bacteria and was in accordance with the MIC and MBC results (Thongsrikhem, Taokaew, Sriariyanun, & Kirdponpattara, 2022). The antibacterial activity of cinnamaldehyde-loaded emulsions slowly decreased over time. After 28 days of storage, the diameters of inhibition zones remained 9.84±0.12 mm and 9.78±0.19 mm for *S. aureus* and *E. coli*, respectively. It indicated the controlled release of cinnamaldehyde from the emulsion droplets, which could contribute to the prolonged antibacterial activity compared to the unencapsulated cinnamaldehyde (Donsì, et al., 2016).

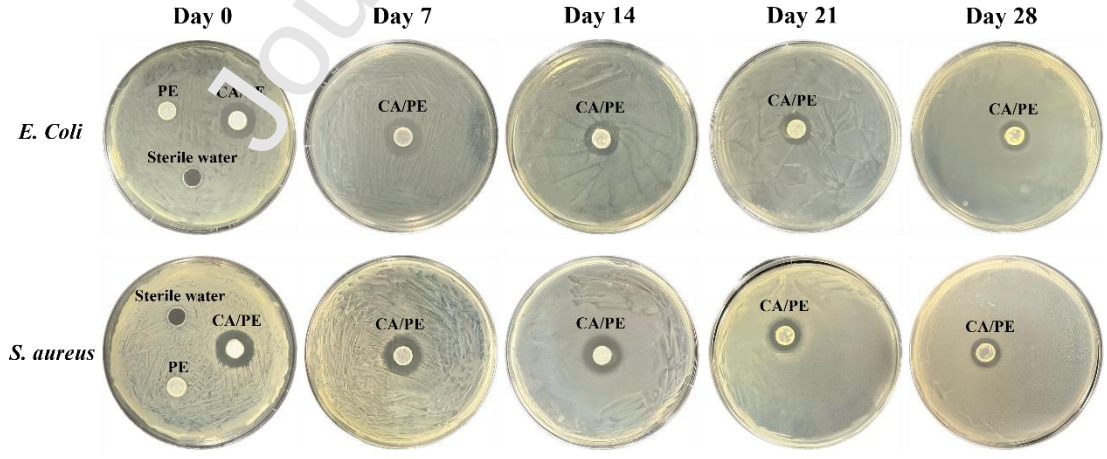

Fig. 5. Zone of inhibition antibacterial test for sterile water, CNC I-0.5 OSA stabilized Pickering emulsions (PE), and PE with encapsulated cinnamaldehyde (CA/PE) during storage at 25°C for 28 days against *E. coli* and *S. aureus* bacteria.

Table 4. Diameter of inhibition zone for cinnamaldehyde-loaded Pickering emulsion stabilized by CNC I-0.5 OSA during storage at 25°C for 28 days against *E. coli* and *S. aureus* bacteria.

Storage time (day)	Diameter of inhibition zone (mm)	
	E. coli	*S. aureus*
0	11.71 ± 0.18^{c}	12.78 ± 0.30^{d}
7	11.36 ± 0.06^{c}	11.67 ± 0.31^{c}
14	10.89 ± 0.13^{b}	12.16 ± 0.14^{cd}
21	10.10 ± 0.26^{a}	10.54 ± 0.48^{b}
28	9.78 ± 0.19^{a}	9.84 ± 0.12^{a}

Notes: Different letters represent statistically significant difference ($p<0.05$).

3.5. Preservation of shrimp

Pseudomonas spp. (Gram-negative bacteria) is known as the dominant cause of the shrimp spoilage during low temperature storage (Don, Xavier, Devi, Nayak, & Kannuchamy, 2018; Lin, et al., 2022). As shown in Fig. 6A, *P. aeruginosa* count value for the control sample (without treatment) increased rapidly during cold storage and reached around 7.4 log CFU/g after 10 days. On day 1, the sample treated with cinnamaldehyde alone had the lowest *P. aeruginosa* count. It was because of the high initial concentration of cinnamaldehyde that could retard the proliferation of *P. aeruginosa* (Rieger, et al., 2014). At day 3, the shrimp sample treated with the cinnamaldehyde-loaded emulsion showed the similar inhibition effect on *P. aeruginosa* compared to cinnamaldehyde alone, and the lowest count value of 6.2 log

CFU/g was revealed after 10 days of storage with the emulsion treatment.

The general microbiological quality is commonly used to evaluate the remaining shelf-life of shrimp (Nazari, et al., 2019). The microbial changes in total viable count (TVC) and psychrophilic bacteria count (PBC) in shrimp samples for 15 days of storage at 4°C are shown in Figs. 6B and 6C, respectively. The TVC and PBC in the control sample (without treatment) increased rapidly from day 3 and exceeded 6 log CFU/g after 6 days of storage. With the coating of cinnamaldehyde-loaded emulsion, the TVC values of shrimp sample increased slightly during the first 6 days of storage and were significantly lower than those of the control sample during the whole storage period. Especially, the sample treated with emulsion had the TVC values of about 5.68 and 6.26 log CFU/g on day 9 and day 12, respectively, which were comparable to that of 6.03 log CFU/g for shrimp packed with active polyethylene films containing rosemary and cinnamon essential oils after 10 days of storage (Dong, Xu, Ahmed, Li, & Lin, 2018). Similarly, the PBC values of shrimp treated with cinnamaldehyde-loaded emulsion were much lower than those of the control and were around 5.9 and 6.6 log CFU/g after 9 and 12 days of storage, respectively, which were lower than that of 6.83 log CFU/g for shrimp coated with alginate and chitosan with grapefruit seed extract after 9 days of storage at 4°C (Kim, Hong, & Oh, 2018). International Commission on Microbiological Specifications for Foods (ICMSF) indicates a bacterial load of 7 log CFU/g as the limit for untreated frozen shrimps. It was worth noting that the TVC and PBC values of shrimp sample with coatings of cinnamaldehyde-loaded emulsion were both lower than 7 log CFU/g after storage at

4°C for 12 days. It suggested that the cinnamaldehyde-loaded emulsion could effectively slow down the growth of bacteria and extend the shelf life of shrimp (Olatunde, et al., 2021; Shiekh, Benjakul, & Sae-leaw, 2019).

Melanosis in shrimp is triggered by polyphenol oxidase (PPO) and lowers the market-value of shrimp. PPO oxidizes phenols into quinones, followed by the non-enzymatic polymerization of quinones, resulting in the formation of black pigments (Arancibia, López-Caballero, Gómez-Guillén, & Montero, 2015). Figs. 6D and 6E show the black spot formation in shrimp samples during storage at 4°C for 15 days. The shrimps coated with cinnamaldehyde-loaded emulsion exhibited obviously lower melanosis scores than the control sample, suggesting the efficiency of cinnamaldehyde-loaded emulsion as a natural preservative to inhibit the melanosis of shrimp. Cinnamaldehyde essential oil could act as a noncompetitive inhibitor for PPO via the reaction of the aldehyde groups in cinnamaldehyde with the amino groups in PPO, resulting in the inhibitory activity against the formation of melanosis in shrimp and the browning in button mushrooms (Gao, Feng, & Jiang, 2014; Mu, Chen, Fang, Mao, & Gao, 2012).

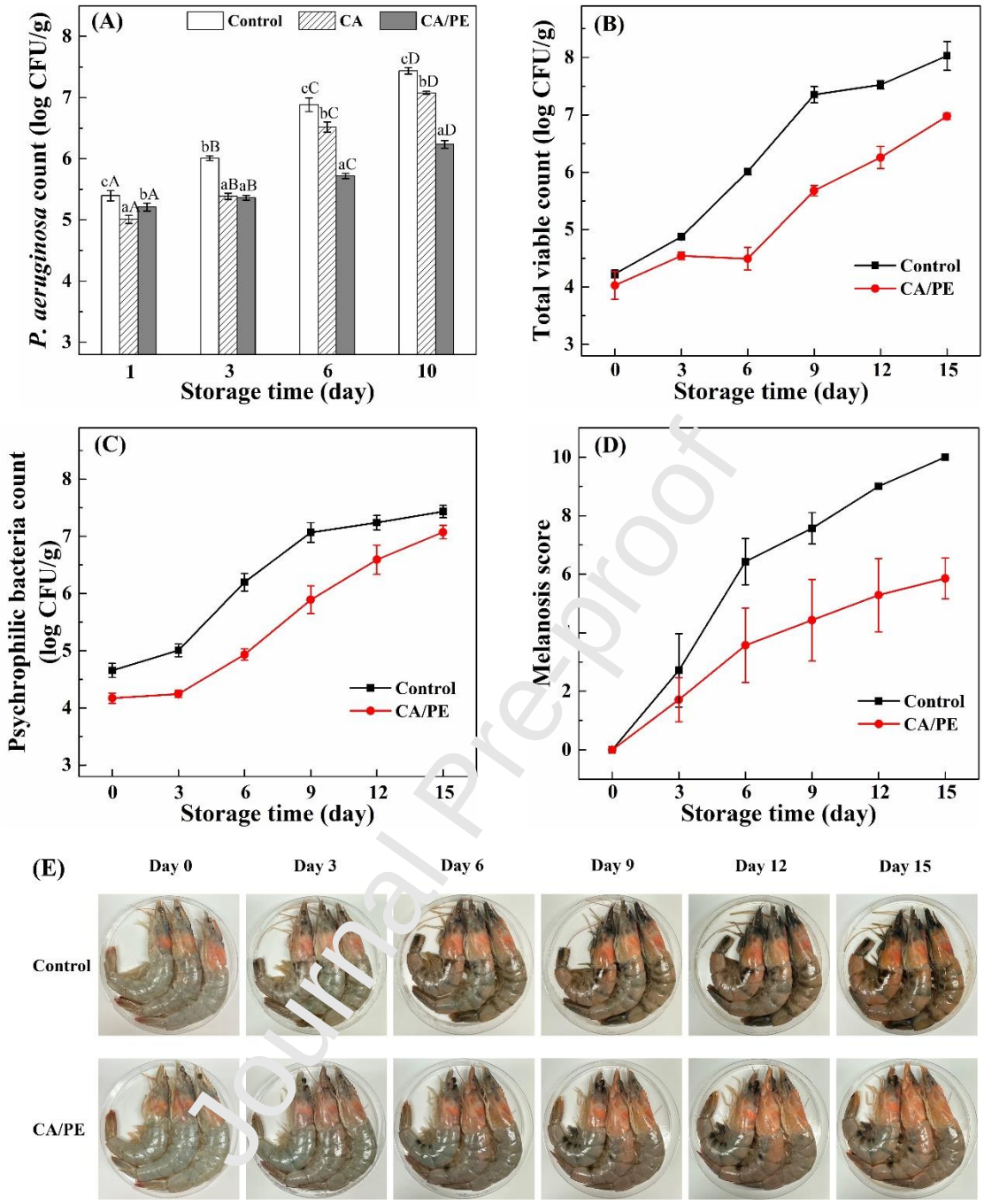

Fig. 6 (A) Changes in *P. aeruginosa* count of shrimp without treatment (Control), shrimp treated with cinnamaldehyde alone (CA), and shrimp treated with cinnamaldehyde-loaded Pickering emulsion stabilized by CNC I-0.5 OSA (CA/PE) during storage at 4°C for 15 days. Different lowercase letters represent statistically significant difference within the same storage time (p<0.05). Different uppercase letters represent statistically significant difference within the same treatment group

(p<0.05). Changes in total viable count (B), psychrophilic bacteria count (C), and melanosis score (D), and photos (E) of shrimp treated without (Control) and with cinnamaldehyde-loaded Pickering emulsion stabilized by CNC I-0.5 OSA (CA/PE) during storage at 4°C for 15 days.

4. CONCLUSIONS

The hypothesis has been confirmed by successfully extracting CNC I and II from Canadian waste maple leaves, which exhibited typical rod-like morphology with aspect ratios of around 17.6 and 10.5, respectively. OSA modification remarkably improved the emulsification performance of CNC I and II, and the CNC I-0.5 OSA particles exhibited excellent emulsifying capacity and stability. The network formed by CNC I-0.5 OSA at oil-water interface increased the surface charge of emulsion droplets and provided physical protection to prevent the droplets from coalescence. The obtained Pickering emulsion showed good encapsulation performance and enhanced storage stability for cinnamaldehyde with 52% remaining after 28 days. The long-term antibacterial activity of cinnamaldehyde-loaded emulsions contributed to the inhibitory effect on the growth of both Gram-positive and Gram-negative bacteria during storage and significantly extended the shelf life of fresh shrimp. Therefore, this work provides new insights into the potential for value-added utilization of maple leaves and the emulsification capacities of surface modified CNC I and II. Moreover, the strategy of spray coating with antibacterial agent-loaded Pickering emulsions is

promising for the preservation of shrimp and other food products.

CRediT authorship contribution statement

Chuye Ji: Conceptualization; Methodology; Investigation; Writing - original draft, review and editing.

Jiachen Wei: Investigation.

Yixiang Wang: Conceptualization; Methodology; Resources; Writing - review and editing; Supervision.

Declaration of competing interest

The authors declare no competing financial interest.

Acknowledgments

The work was supported by the Natural Sciences and Engineering Research Council of Canada (NSERC RGPIN-2019-04498, NSERC DGECR-2019-00472). C. J. would like to thank the support of China Scholarship Council (CSC NO. 202106790028).

References

Andrews, J. M. (2001). Determination of minimum inhibitory concentrations. *Journal of Antimicrobial Chemotherapy, 48*(suppl_1), 5-16. https://doi.org/10.1093/jac/48.suppl_1.5.

Arancibia, M. Y., López-Caballero, M. E., Gómez-Guillén, M. C., & Montero, P. (2015). Chitosan coatings enriched with active shrimp waste for shrimp preservation. *Food Control, 54*, 259-266. https://doi.org/10.1016/j.foodcont.2015.02.004.

Azubuike, C. P., Rodríguez, H., Okhamafe, A. O., & Rogers, R. D. (2012).

Physicochemical properties of maize cob cellulose powders reconstituted from ionic liquid solution. *Cellulose, 19*(2), 425-433. https://doi.org/10.1007/s10570-011-9631-y.

Binks, B. P. (2002). Particles as surfactants—similarities and differences. *Current opinion in colloid & interface science, 7*(1), 21-41. https://doi.org/10.1016/S1359-0294(02)00008-0.

Chen, H., McClements, D. J., Chen, E., Liu, S., Li, P., & Li, Y. (2017). *In situ* interfacial conjugation of chitosan with cinnamaldehyde during homogenization improves the formation and stability of chitosan-stabilized emulsions. *Langmuir, 33*(51), 14608-14617. https://doi.org/10.1021/acs.langmuir.7b03852.

Chen, J., Li, S., Zheng, Q., Feng, X., Tan, W., Feng, K., Liu, Y., & Hu, W. (2022). Preparation of solid lipid nanoparticles of cinnamaldehyde and determination of sustained release capacity. *Nanomaterials, 12*(24), 4460. https://doi.org/10.3390/nano12244460.

Chen, Q.-H., Zheng, J., Xu, Y.-T., Yin, S.-W., Liu, F., & Tang, C.-H. (2018). Surface modification improves fabrication of pickering high internal phase emulsions stabilized by cellulose nanocrystals. *Food Hydrocolloids, 75*, 125-130. https://doi.org/10.1016/j.foodhyd.2017.09.005.

Cheng, H., Khan, M. A., Xie, Z., Tao, S., Li, Y., & Liang, L. (2020). A peppermint oil emulsion stabilized by resveratrol-zein-pectin complex particles: Enhancing the chemical stability and antimicrobial activity in combination with the

synergistic effect. *Food Hydrocolloids, 103*, 105675. https://doi.org/10.1016/j.foodhyd.2020.105675.

Cherhal, F., Cousin, F., & Capron, I. (2016). Structural description of the interface of Pickering emulsions stabilized by cellulose nanocrystals. *Biomacromolecules, 17*(2), 496-502. https://doi.org/10.1021/acs.biomac.5b01413.

Cocchiara, J., Letizia, C. S., Lalko, J., Lapczynski, A., & Api, A. M. (2005). Fragrance material review on cinnamaldehyde. *Food and Chemical Toxicology, 43*(6), 867-923. https://doi.org/10.1016/j.fct.2004.09.014.

Corrêa, A. C., de Morais Teixeira, E., Pessan, L. A., & Mattoso, L. H. C. (2010). Cellulose nanofibers from curaua fibers. *Cellulose, 17*(6), 1183-1192. https://doi.org/10.1007/s10570-010-9453-3.

Dai, H., Wu, J., Zhang, H., Chen, Y., Ma, L., Huang, H., Huang, Y., & Zhang, Y. (2020). Recent advances on cellulose nanocrystals for Pickering emulsions: Development and challenge. *Trends in Food Science & Technology, 102*, 16-29. https://doi.org/10.1016/j.tifs.2020.05.016.

Dai, H., Zhang, H., Chen, Y., Ma, L., Wu, J., & Zhang, Y. (2021). Co-stabilization and properties regulation of Pickering emulsions by cellulose nanocrystals and nanofibrils from lemon seeds. *Food Hydrocolloids, 120*, 106884. https://doi.org/10.1016/j.foodhyd.2021.106884.

Domingues, M. M., Silva, P. M., Franquelim, H. G., Carvalho, F. A., Castanho, M. A. R. B., & Santos, N. C. (2014). Antimicrobial protein rBPI21-induced surface changes on Gram-negative and Gram-positive bacteria. *Nanomedicine:*

Nanotechnology, Biology and Medicine, 10(3), 543-551. https://doi.org/10.1016/j.nano.2013.11.002.

Don, S., Xavier, K. A. M., Devi, S. T., Nayak, B. B., & Kannuchamy, N. (2018). Identification of potential spoilage bacteria in farmed shrimp (*Litopenaeus vannamei*): Application of relative rate of spoilage models in shelf life-prediction. *LWT, 97*, 295-301. https://doi.org/10.1016/j.lwt.2018.07.006.

Dong, Z., Xu, F., Ahmed, I., Li, Z., & Lin, H. (2018). Characterization and preservation performance of active polyethylene films containing rosemary and cinnamon essential oils for Pacific white shrimp packaging. *Food Control, 92*, 37-46. https://doi.org/10.1016/j.foodcont.2018.04.052.

Donsì, F., & Ferrari, G. (2016). Essential oil nanoemulsions as antimicrobial agents in food. *Journal of Biotechnology, 233*, 106-120. https://doi.org/10.1016/j.jbiotec.2016.07.005.

Du Le, H., Loveday, S. M., Singh, H., & Sarkar, A. (2020). Pickering emulsions stabilised by hydrophobically modified cellulose nanocrystals: Responsiveness to pH and ionic strength. *Food Hydrocolloids, 99*, 105344. https://doi.org/10.1016/j.foodhyd.2019.105344.

Flauzino Neto, W. P., Putaux, J.-L., Mariano, M., Ogawa, Y., Otaguro, H., Pasquini, D., & Dufresne, A. (2016). Comprehensive morphological and structural investigation of cellulose I and II nanocrystals prepared by sulphuric acid hydrolysis. *RSC Advances, 6*(79), 76017-76027. https://doi.org/10.1039/C6RA16295A.

Foo, M. L., Ooi, C. W., Tan, K. W., & Chew, I. M. L. (2022). Preparation of black cumin seed oil Pickering nanoemulsion with enhanced stability and antioxidant potential using nanocrystalline cellulose from oil palm empty fruit bunch. *Chemosphere, 287*, 132108. https://doi.org/10.1016/j.chemosphere.2021.132108.

French, A. D. (2014). Idealized powder diffraction patterns for cellulose polymorphs. *Cellulose, 21*(2), 885-896. https://doi.org/10.1007/s10570-013-0030-4.

French, A. D., & Santiago Cintrón, M. (2013). Cellulose polymorphy, crystallite size, and the Segal Crystallinity Index. *Cellulose, 20*(1), 583-588. https://doi.org/10.1007/s10570-012-9863-y.

Gao, K., Liu, Y., Liu, T., Song, X., Duan, R., Feng, S., Wang, X., & Cui, X. (2022). OSA improved the stability and applicability of emulsions prepared with enzymatically hydrolyzed pomelo peel insoluble fiber. *Food Hydrocolloids, 132*, 107806. https://doi.org/10.1016/j.foodhyd.2022.107806.

Gao, M., Feng, L., & Jiang, T. (2014). Browning inhibition and quality preservation of button mushroom (*Agaricus bisporus*) by essential oils fumigation treatment. *Food Chemistry, 149*, 107-113. https://doi.org/10.1016/j.foodchem.2013.10.073.

García-García, D., Balart, R., Lopez-Martinez, J., Ek, M., & Moriana, R. (2018). Optimizing the yield and physico-chemical properties of pine cone cellulose nanocrystals by different hydrolysis time. *Cellulose, 25*(5), 2925-2938. https://doi.org/10.1007/s10570-018-1760-0.

Gong, J., Mo, L., & Li, J. (2018). A comparative study on the preparation and characterization of cellulose nanocrystals with various polymorphs. *Carbohydrate Polymers, 195*, 18-28. https://doi.org/10.1016/j.carbpol.2018.04.039.

Gottenbos, B., Grijpma, D. W., van der Mei, H. C., Feijen, J., & Busscher, H. J. (2001). Antimicrobial effects of positively charged surfaces on adhering Gram-positive and Gram-negative bacteria. *Journal of Antimicrobial Chemotherapy, 48*(1), 7-13. https://doi.org/10.1093/jac/48.1.7.

Han, J., Zhou, C., Wu, Y., Liu, F., & Wu, Q. (2013). Self-assembling behavior of cellulose nanoparticles during freeze-drying: Effect of suspension concentration, particle size, crystal structure, and surface charge. *Biomacromolecules, 14*(5), 1529-1540. https://doi.org/10.1021/bm4001734.

Han, Y., Ding, J., Zhang, J., Li, Q., Yang, H., Sun, T., & Li, H. (2021). Fabrication and characterization of polylactic acid coaxial antibacterial nanofibers embedded with cinnamaldehyde/tea polyphenol with food packaging potential. *International journal of biological macromolecules, 184*, 739-749. https://doi.org/10.1016/j.ijbiomac.2021.06.143.

Haouache, S., Chen, Y., Jimenez-Saelices, C., Cousin, F., Chen, P., Nishiyama, Y., Jerome, F., & Capron, I. (2022a). Edge-on (cellulose II) and face-on (cellulose I) adsorption of cellulose nanocrystals at the oil–water interface: A combined entropic and enthalpic process. *Biomacromolecules, 23*(9), 3517-3524. https://doi.org/10.1021/acs.biomac.2c00201.

Haouache, S., Jimenez-Saelices, C., Cousin, F., Falourd, X., Pontoire, B., Cahier, K., Jérome, F., & Capron, I. (2022b). Cellulose nanocrystals from native and mercerized cotton. *Cellulose, 29*(3), 1567-1581. https://doi.org/10.1007/s10570-021-04313-8.

Huang, S., Liu, X., Chang, C., & Wang, Y. (2020). Recent developments and prospective food-related applications of cellulose nanocrystals: a review. *Cellulose, 27*(6), 2991-3011. https://doi.org/10.1007/s10570-020-02984-3.

Ruan H., Chen Q., Fu M., Xu Q., & He G. (2009) Preparation and properties of octenyl succinic anhydride modified potato starch. *Food Chemistry, 114*(1), 81-86. https://doi.org/10.1016/j.foodchem.2008.09.019.

Ibrahim Sallam, K. (2007). Antimicrobial and antioxidant effects of sodium acetate, sodium lactate, and sodium citrate in refrigerated sliced salmon. *Food Control, 18*(5), 566-575. https://doi.org/10.1016/j.foodcont.2006.02.002.

Javidi, F., Razavi, S. M. A., & Mohammad Amini, A. (2019). Cornstarch nanocrystals as a potential fat replacer in reduced fat O/W emulsions: A rheological and physical study. *Food Hydrocolloids, 90*, 172-181. https://doi.org/10.1016/j.foodhyd.2018.12.003.

Jo, Y.-J., Chun, J.-Y., Kwon, Y.-J., Min, S.-G., Hong, G.-P., & Choi, M.-J. (2015). Physical and antimicrobial properties of trans-cinnamaldehyde nanoemulsions in water melon juice. *LWT - Food Science and Technology, 60*(1), 444-451. https://doi.org/10.1016/j.lwt.2014.09.041.

Kalashnikova, I., Bizot, H., Cathala, B., & Capron, I. (2012). Modulation of cellulose

nanocrystals amphiphilic properties to stabilize oil/water interface. *Biomacromolecules, 13*(1), 267-275. https://doi.org/10.1021/bm201599j.

Kargarzadeh, H., Ahmad, I., Abdullah, I., Dufresne, A., Zainudin, S. Y., & Sheltami, R. M. (2012). Effects of hydrolysis conditions on the morphology, crystallinity, and thermal stability of cellulose nanocrystals extracted from kenaf bast fibers. *Cellulose, 19*(3), 855-866. https://doi.org/10.1007/s10570-012-9684-6.

Kim, J.-H., Hong, W.-s., & Oh, S.-W. (2018). Effect of layer-by-layer antimicrobial edible coating of alginate and chitosan with grapefruit seed extract for shelf-life extension of shrimp (*Litopenaeus vannamei*) stored at 4 °C. *International journal of biological macromolecules, 120*, 1468-1473. https://doi.org/10.1016/j.ijbiomac.2018.09.160.

Ko, E. B., & Kim, J.-Y. (2021). Application of starch nanoparticles as a stabilizer for Pickering emulsions: Effect of environmental factors and approach for enhancing its storage stability. *Food Hydrocolloids, 120*, 106984. https://doi.org/10.1016/j.foodhyd.2021.106984.

Ko, S. W., Soriano, J. P. E., Rajan Unnithan, A., Lee, J. Y., Park, C. H., & Kim, C. S. (2018). Development of bioactive cellulose nanocrystals derived from dominant cellulose polymorphs I and II from *Capsosiphon Fulvescens* for biomedical applications. *International journal of biological macromolecules, 110*, 531-539. https://doi.org/10.1016/j.ijbiomac.2017.11.047.

Li, P., Li, J., Feng, X., Li, J., Hao, Y., Zhang, J., Wang, H., Yin, A., Zhou, J., Ma, X.,

& Wang, B. (2019). Metal-organic frameworks with photocatalytic bactericidal activity for integrated air cleaning. *Nature Communications, 10*(1), 2177. https://doi.org/10.1038/s41467-019-10218-9.

Li, X., Li, J., Gong, J., Kuang, Y., Mo, L., & Song, T. (2018). Cellulose nanocrystals (CNCs) with different crystalline allomorph for oil in water Pickering emulsions. *Carbohydrate Polymers, 183*, 303-310. https://doi.org/10.1016/j.carbpol.2017.12.085.

Li, Y., Lei, Y., Tan, Y., Zhang, J., Hong, H., & Luo, Y. (2022). Efficacy of freeze-chilled storage combined with tea polyphenol for controlling melanosis, quality deterioration, and spoilage bacterial growth of Pacific white shrimp (*Litopenaeus vannamei*). *Food Chemistry, 370*, 130924. https://doi.org/10.1016/j.foodchem.2021.130924.

Li, Y., Li, G., Zou, Y., Zhou, Q., & Lian, X. (2014). Preparation and characterization of cellulose nanofibers from partly mercerized cotton by mixed acid hydrolysis. *Cellulose, 21*(1), 301-309. https://doi.org/10.1007/s10570-013-0146-6.

Lin, D., Sun, L.-C., Chen, Y.-L., Liu, G.-M., Miao, S., & Cao, M.-J. (2022). Shrimp spoilage mechanisms and functional films/coatings used to maintain and monitor its quality during storage. *Trends in Food Science & Technology, 129*, 25-37. https://doi.org/10.1016/j.tifs.2022.08.020.

Liu, C. F., Sun, R. C., Zhang, A. P., Ren, J. L., & Geng, Z. C. (2006). Structural and thermal characterization of sugarcane bagasse cellulose succinates prepared in

ionic liquid. *Polymer Degradation and Stability, 91*(12), 3040-3047. https://doi.org/10.1016/j.polymdegradstab.2006.08.004.

Lu, H., & Tian, Y. (2021). Nanostarch: Preparation, modification, and application in Pickering emulsions. *Journal of Agricultural and Food Chemistry, 69*(25), 6929-6942. https://doi.org/10.1021/acs.jafc.1c01244.

Melgosa, R., Benito-Román, Ó., Sanz, M. T., de Paz, E., & Beltrán, S. (2019). Omega–3 encapsulation by PGSS-drying and conventional drying methods. Particle characterization and oxidative stability. *Food Chemistry, 270*, 138-148. https://doi.org/10.1016/j.foodchem.2018.07.082.

Miao, M., Li, R., Jiang, B., Cui, S. W., Zhang, T., & Jin, Z. (2014). Structure and physicochemical properties of octenyl succinic esters of sugary maize soluble starch and waxy maize starch. *Food Chemistry, 151*, 154-160. https://doi.org/10.1016/j.foodchem.2013.11.043.

Mikulcová, V., Bordes, R., & Kašpárková, V. (2016). On the preparation and antibacterial activity of emulsions stabilized with nanocellulose particles. *Food Hydrocolloids, 61*, 780-792. https://doi.org/10.1016/j.foodhyd.2016.06.031.

Mu, H., Chen, H., Fang, X., Mao, J., & Gao, H. (2012). Effect of cinnamaldehyde on melanosis and spoilage of Pacific white shrimp (*Litopenaeus vannamei*) during storage. *Journal of the Science of Food and Agriculture, 92*(10), 2177-2182. https://doi.org/10.1002/jsfa.5605.

Muhoza, B., Qi, B., Harindintwali, J. D., Koko, M. Y. F., Zhang, S., & Li, Y. (2023).

Encapsulation of cinnamaldehyde: an insight on delivery systems and food applications. *Critical reviews in food science and nutrition*, *63*, 2521-2543. https://doi.org/10.1080/10408398.2021.1977236.

Nazari, M., Majdi, H., Milani, M., Abbaspour-Ravasjani, S., Hamishehkar, H., & Lim, L.-T. (2019). Cinnamon nanophytosomes embedded electrospun nanofiber: Its effects on microbial quality and shelf-life of shrimp as a novel packaging. *Food Packaging and Shelf Life 21*, 100349. https://doi.org/10.1016/j.fpsl.2019.100349.

Nirmal, N. P., & Benjakul, S. (2009). Melanosis and quality changes of Pacific white shrimp (*Litopenaeus vannamei*) treated with catechin during iced storage. *Journal of Agricultural and Food Chemistry, 57*(9), 3578-3586. https://doi.org/10.1021/jf900051e.

Olatunde, O. O., Tan, S. L. D., Shiekh, K. A., Benjakul, S., & Nirmal, N. P. (2021). Ethanolic guava leaf extracts with different chlorophyll removal processes: Anti-melanosis, antibacterial properties and the impact on qualities of Pacific white shrimp during refrigerated storage. *Food Chemistry, 341*, 128251. https://doi.org/10.1016/j.foodchem.2020.128251.

Pang, B., Zhang, H., Schilling, M., Liu, H., Wang, X., Rehfeldt, F., & Zhang, K. (2020). High-internal-phase Pickering emulsions stabilized by polymeric dialdehyde cellulose-based nanoparticles. *ACS Sustainable Chemistry & Engineering, 8*(19), 7371-7379. https://doi.org/10.1021/acssuschemeng.0c01116.

Quintero-Castaño, V. D., Castellanos-Galeano, F. J., Álvarez-Barreto, C. I., Lucas-Aguirre, J. C., Bello-Pérez, L. A., & Rodríguez-Garcia, M. E. (2020). Starch from two unripe plantains and esterified with octenyl succinic anhydride (OSA): Partial characterization. *Food Chemistry, 315*, 126241. https://doi.org/10.1016/j.foodchem.2020.126241.

Rieger, K. A., & Schiffman, J. D. (2014). Electrospinning an essential oil: Cinnamaldehyde enhances the antimicrobial efficacy of chitosan/poly(ethylene oxide) nanofibers. *Carbohydrate Polymers, 113*, 561-568. https://doi.org/10.1016/j.carbpol.2014.06.075.

Sae-leaw, T., & Benjakul, S. (2019). Prevention of quality loss and melanosis of Pacific white shrimp by cashew leaf extracts. *Food Control, 95*, 257-266. https://doi.org/10.1016/j.foodcont.2018.08.014.

Sarko, A., & Muggli, R. (1974). Packing analysis of carbohydrates and polysaccharides. III. Valonia cellulose and cellulose II. *Macromolecules, 7*(4), 486-494.

Schenzel, K., Almlöf, H., & Germgård, U. (2009). Quantitative analysis of the transformation process of cellulose I → cellulose II using NIR FT Raman spectroscopy and chemometric methods. *Cellulose, 16*(3), 407-415. https://doi.org/10.1007/s10570-009-9286-0.

Shen, S., Zhang, T., Yuan, Y., Lin, S., Xu, J., & Ye, H. (2015). Effects of cinnamaldehyde on *Escherichia coli* and *Staphylococcus aureus* membrane. *Food Control, 47*, 196-202. https://doi.org/10.1016/j.foodcont.2014.07.003.

Shi, C., Zhang, X., Zhao, X., Meng, R., Liu, Z., Chen, X., & Guo, N. (2017). Synergistic interactions of nisin in combination with cinnamaldehyde against *Staphylococcus aureus* in pasteurized milk. *Food Control, 71*, 10-16. https://doi.org/10.1016/j.foodcont.2016.06.020.

Shiekh, K. A., Benjakul, S., & Sae-leaw, T. (2019). Effect of Chamuang (*Garcinia cowa Roxb.*) leaf extract on inhibition of melanosis and quality changes of Pacific white shrimp during refrigerated storage. *Food Chemistry, 270*, 554-561. https://doi.org/10.1016/j.foodchem.2018.07.139.

Sweedman, C. M., Tizzotti J. M., Schäfer C., & Gilbert G. R. (2013). Structure and physicochemical properties of octenyl succinic anhydride modified starches: A review. *Carbohydrate Polymers, 92*(1), 905-920. https://doi.org/10.1016/j.carbpol.2012.09.040.

Takihara, T., Yoshida, Y., & Isogai, A. (2007). Reactions between cellulose diacetate and alkenylsuccinic anhydrides and characterization of the reaction products. *Cellulose, 14*(4), 357-366. https://doi.org/10.1007/s10570-007-9112-5.

Tang, C., Chen, Y., Luo, J., Low, M. Y., Shi, Z., Tang, J., Zhang, Z., Peng, B., & Tam, K. C. (2019). Pickering emulsions stabilized by hydrophobically modified nanocellulose containing various structural characteristics. *Cellulose, 26*, 7753-7767. https://doi.org/10.1007/s10570-019-02648-x.

Thongsrikhem, N., Taokaew, S., Sriariyanun, M., & Kirdponpattara, S. (2022). Antibacterial activity in gelatin-bacterial cellulose composite film by thermally crosslinking with cinnamaldehyde towards food packaging

application. *Food Packaging and Shelf Life, 31*, 100766. https://doi.org/10.1016/j.fpsl.2021.100766.

Wang, C., He, X.-W., Huang, Q., Luo, F.-x., & Fu, X. (2013). The mechanism of starch granule reacted with OSA by phase transition catalyst in aqueous medium. *Food Chemistry, 141*(4), 3381-3385. https://doi.org/10.1016/j.foodchem.2013.06.029.

Wang, L., Gao, Y., Li, J., Subirade, M., Song, Y., & Liang, L. (2016). Effect of resveratrol or ascorbic acid on the stability of α-tocopherol in O/W emulsions stabilized by whey protein isolate: Simultaneous encapsulation of the vitamin and the protective antioxidant. *Food Chemistry, 196*, 466-474. https://doi.org/10.1016/j.foodchem.2015.09.071.

Wang, W., Du, G., Li, C., Zhang, H., Long, Y., & Ni, Y. (2016). Preparation of cellulose nanocrystals from asparagus (*Asparagus officinalis L.*) and their applications to palm oil/water Pickering emulsion. *Carbohydrate Polymers, 151*, 1-8. https://doi.org/10.1016/j.carbpol.2016.05.052.

Wang, X., Cheng, F., Wang, X., Feng, T., Xia, S., & Zhang, X. (2021). Chitosan decoration improves the rapid and long-term antibacterial activities of cinnamaldehyde-loaded liposomes. *International journal of biological macromolecules, 168*, 59-66. https://doi.org/10.1016/j.ijbiomac.2020.12.003.

Xie, Y., Liu, H., Li, Y., Tian, J., Qin, X., Shabani, K. I., Liao, C., & Liu, X. (2020). Characterization of Pickering emulsions stabilized by OSA-modified sweet potato residue cellulose: Effect of degree of substitute and concentration. *Food*

Hydrocolloids, 108, 105915. https://doi.org/10.1016/j.foodhyd.2020.105915.

Xing, L., Gu, J., Zhang, W., Tu, D., & Hu, C. (2018). Cellulose I and II nanocrystals produced by sulfuric acid hydrolysis of Tetra pak cellulose I. *Carbohydrate Polymers, 192*, 184-192. https://doi.org/10.1016/j.carbpol.2018.03.042.

Xing, L., Hu, C., Zhang, W., Guan, L., & Gu, J. (2020). Transition of cellulose supramolecular structure during concentrated acid treatment and its implication for cellulose nanocrystal yield. *Carbohydrate Polymers, 229*, 115539. https://doi.org/10.1016/j.carbpol.2019.115539.

Zainal Abiddin, N. F., Yusoff, A., & Ahmad, N. (2018). Effect of octenylsuccinylation on physicochemical, thermal, morphological and stability of octenyl succinic anhydride (OSA) modified sago starch. *Food Hydrocolloids, 75*, 138-146. https://doi.org/10.1016/j.foodhyd.2017.09.003.

Zou, Y., van Baalen, C., Yang, X., & Scholten, E. (2018). Tuning hydrophobicity of zein nanoparticles to control rheological behavior of Pickering emulsions. *Food Hydrocolloids, 80*, 130-140. https://doi.org/10.1016/j.foodhyd.2018.02.014.

Zugenmaier, P. (2001). Conformation and packing of various crystalline cellulose fibers. *Progress in Polymer Science, 26*(9), 1341-1417. https://doi.org/10.1016/S0079-6700(01)00019-3.

Graphical abstract